Vector analyzing powers of deuteron-proton elastic scattering and breakup at 130 MeV

I. Ciepał,[1,*] St. Kistryn,[1] E. Stephan,[2] A. Biegun,[3] K. Bodek,[1] A. Deltuva,[4] E. Epelbaum,[5] M. Eslami-Kalantari,[3] A. Fonseca,[4] J. Golak,[1] V. Jha,[6] N. Kalantar-Nayestanaki,[3] H. Kamada,[7] G. Khatri,[1] Da. Kirillov,[5,8] Di. Kirillov,[8] M. Kiš,[3] St. Kliczewski,[9] B. Kłos,[2] A. Kozela,[9] M. Kravcikova,[10] M. Lesiak,[1,5] H. Machner,[5] A. Magiera,[1,3] G. Martinska,[11] J. Messchendorp,[3] A. Nogga,[5] W. Parol,[1] A. Ramazani-Moghaddam-Arani,[3] B. J. Roy,[6,12] H. Sakai,[13] K. Sekiguchi,[14] I. Sitnik,[8] R. Siudak,[9] R. Skibiński,[1] R. Sworst,[1] J. Urban,[11] H. Witała,[1] A. Wrońska,[1] and J. Zejma[1]

[1]*Institute of Physics, Jagiellonian University, PL-30059 Kraków, Poland*
[2]*Institute of Physics, University of Silesia, PL-40007 Katowice, Poland*
[3]*Kernfysisch Versneller Instituut, University of Groningen, NL-9747 AA Groningen, the Netherlands*
[4]*Centro de Física Nuclear da Universidade de Lisboa, P-1649-003 Lisboa, Portugal*
[5]*Forschungszentrum Jülich, Institut für Kernphysik, D-52425 Jülich, Germany*
[6]*BARC, Bombay 400 085, India*
[7]*Department of Physics, Kyushu Institute of Technology, Kitakyushu 804-8550, Japan*
[8]*JINR, RU-141980 Dubna, Russia*
[9]*Institute of Nuclear Physics, PL-31342 Kraków, Poland*
[10]*Technical University, SK-04101 Kosice, Slovakia*
[11]*P. J. Safarik University, SK-04154 Kosice, Slovakia*
[12]*Universität Bonn, D-53113 Bonn, Germany*
[13]*University of Tokyo, Bunkyo, J-1130033 Tokyo, Japan*
[14]*Tohoku University, Sendai, J-9808578, Japan*

(Received 29 September 2011; published 11 January 2012)

Set of vector analyzing power data of the $\vec{d}p$ elastic scattering and ${}^1H(\vec{d},pp)n$ breakup reactions at 130-MeV deuteron beam energy has been measured in the domain of very forward polar angles. The results are compared with theoretical predictions originating from various approaches: realistic nucleon-nucleon (NN) potentials and the NN potentials combined with a three-nucleon force (3NF) model and with predictions based on the ChPT framework. In case of the breakup process, none of the theoretical calculations reveal sensitivity to any of the dynamical effects such as 3NF or Coulomb interaction and they describe the experimental data equally well. For the elastic scattering, the Coulomb correction appears not negligible at very small $\theta_d^{\text{c.m.}}$. The effect seems to be confirmed by the data.

DOI: 10.1103/PhysRevC.85.017001 PACS number(s): 21.30.−x, 24.70.+s, 25.10.+s, 13.75.Cs

Few-nucleon systems are microscopic laboratories most suited for detailed study of the nucleon-nucleon (NN) interaction dynamics and the nuclear forces. Among them, the system composed of three nucleons (3N) is the simplest nontrivial environment where NN force models can be tested. Properties of 3N systems at medium energies are mainly determined by pairwise NN interaction. There are, however, reasons to assume the existence of additional dynamical effects like three-nucleon force (3NF) related to the presence of the third nucleon, or the Coulomb interaction, very significant in the domain of small polar angles of the emitted protons. Both effects are modeled within different theoretical formalisms.

The realistic two-nucleon (2N) forces can be combined with the recent version of the 2π-exchange Tucson-Melbourne (TM) 3NF [1] or in the case of AV18 NN force with the Urbana IX 3NF [2]. Alternatively, 3NF can be generated by an explicit treatment of the Δ isobar excitation within the coupled channel (CC) method [3]. For the 3N system, creation of a Δ-containing state yields an effective 3NF but also two-barion dispersion. These two effects usually compete, and therefore the net effects of including the Δ isobar in the potential are smaller than for approaches with the phenomenological 3NF's. When the chiral perturbation theory (ChPT) is used at the next-to-next-to-leading order (NNLO), the 3N contributions arise naturally, fully consistently with the NN force terms [4].

The long-range electromagnetic component of the NN interaction was successfully implemented in CC formalism [5,6] as well as in the calculations [7] based on the AV18 NN potential combined with the Urbana IX 3NF.

Besides the binding energies of the light nuclei, the importance of the 3NF was experimentally confirmed on the basis of the data originating from the nucleon-deuteron elastic scattering process [8–17]. In general, inclusion of the 3NF component improves the description of the cross-sectional data. However, quite significant discrepancies between the theoretical models and polarization observables are still present. Exploration of the nucleon-deuteron breakup can be considered as a natural next step in the investigations of the few-nucleon system dynamics. The reaction offers a very rich basis for verifying and developing the interaction models. Experimental data for the cross section for the ${}^1H(d,pp)n$ breakup reaction at 130 MeV [18–20] not only proved the importance of the 3NF but also revealed new unexpected effects due to the electromagnetic part of the interaction. These

*izabela.ciepal@uj.edu.pl

findings were a clue for further investigations of the Coulomb force in the cross sections and polarization observables in a very forward angular region of the outgoing protons.

The experiments were carried out with the use of the COSY (COoler SYnchrotron) accelerator and the Germanium Wall (GeWall) detector [21] at the Research Center in Jülich. The 130-MeV deuteron beam has been produced in the polarized ion source (colliding beam source type). We used the beam in two states: transversally vector polarized $(P_z, P_{zz}) = (-\frac{2}{3}, 0)$ and unpolarized $(P_z, P_{zz}) = (0, 0)$. The paper presents vector analyzing powers for the breakup and elastic scattering processes.

The GeWall detection system was one of the external facilities, using the extracted COSY beam. For such experiments, one of the serious problems in obtaining a beam with very good properties is beam-halo existence, which induces substantial background. To suppress this effect, electron cooling was used during the acceleration process. The extracted deuteron beam was finally focused on a liquid hydrogen target 2 mm thick with a spot described by $\sigma \approx 1.0$ mm. However, the tails of the direct beam were still present on the detector. Therefore, the experiment utilized a veto counter, which limited the acceptance of the beam to its intense core. The products of the reactions of interest were measured by the GeWall setup, which consisted of three high-purity semiconductor position-sensitive germanium detectors. Each detector possessed a central hole to allow the beam particles that did not interact with the target to be dumped further downstream. Two different types of detectors were used: a thin transmission detector "Quirl" with an excellent spatial resolution and two thick energy detectors $E1$ and $E2$ with excellent energy resolutions. Dimensions of the holes, the total diameters of the detectors, and the distances from the target define the angular acceptance of the detection system, which was 3–14° for the polar and 2π for the azimuthal angles.

The Quirl detector was used to determine the position and the energy loss (ΔE detector) of the passing charged particles. It was segmented on the front and the rear sides to 2×200 grooves, shaped as Archimedes spirals, each covering an angular range of 2π (including the central hole region). The bending direction of the spirals on the front and rear sides were opposite to each other. Thus, the overlaps of the spirals formed an array of about 20 000 pixels.

The energy detectors $E1$ and $E2$ were divided into 32 wedge-like segments each and mainly used for measuring energies of the charged reaction products as well as providing additional azimuthal information.

Information on energy losses in different GeWall components is used for particle identification, whereas the sum of these energies gives the total kinetic energy of the particle. Position information from the Quirl detector enables the determination of all components of the momentum vector of the particle (assuming a pointlike interaction region at the target); the distance from the target and the position on Quirl transform directly to the azimuthal angle ϕ and the polar angle θ.

The very first step of the data analysis was event selection. The $\Delta E - E$ technique allowed for very clear separation of the elastic events from the breakup protons. The events of interest, which can be distinguished within the acceptance of the GeWall detector, are the coincidences of two protons from the breakup reaction, and the elastic events. The elastic scattering events, depending on the range of polar angles, can be identified as single-track events (protons or deuterons) or deuteron-proton coincidences (two-track events). In the case of analysis of the coincident events, the direct beam deuterons responsible for the accidental coincidences (especially for very small polar angles $\theta < 7^\circ$) were eliminated by kinematical conditions. The elastically scattered protons and deuterons, registered as single particles, were used for determination of the beam polarization. For such events, the background of direct beam was subtracted and the systematic uncertainties related to that procedure were estimated to be about 1.5%.

In order to study the polarization observables, the numbers of the elastically scattered deuterons and protons at given polar angle θ and azimuthal angle φ for polarized $(P_z, P_{zz}) = (-\frac{2}{3}, 0)$ and unpolarized $(P_z, P_{zz}) = (0, 0)$ beam states were obtained. They have been relatively normalized to the beam current, corrected for the dead time, and scaled by an adequate trigger factor. On their basis, a ratio $f^\theta(\varphi)$ was constructed:

$$f^\theta(\varphi) = \frac{N^\theta_{\text{pol}} - N^\theta_0}{N^\theta_0}, \tag{1}$$

where N^θ_{pol} and N^θ_0 denote final numbers of events evaluated for the polarized and unpolarized beam, respectively. In the ratio, all factors constant in time (e.g., target thickness, detection efficiency, etc.) are canceled.

Because only pure vector beam polarization state was available in the experiment, the number of the elastically scattered events N^θ_{pol} obtained for the polarized state is described by a formula:

$$N^\theta_{\text{pol}}(\varphi) = N^\theta_0 \cdot [1 + iT_{11}(\theta)\sqrt{3}P_z \cos\varphi], \tag{2}$$

where $iT_{11}(\theta)$ are spherical vector analyzing powers. Substituting the formula (2) into Eq. (1) allows us to obtain the final expression for the theoretical dependency $f^\theta(\varphi)$ as a function of the angle φ:

$$f^\theta(\varphi) = iT_{11}(\theta)P_z\sqrt{3}\cos\varphi. \tag{3}$$

Fit of the function given in Eq. (3) to the experimental $f^\theta(\varphi)$ distribution can be used to obtain polarization values if the analyzing powers are known, or vice versa: With the known polarization values one is able to extract the analyzing powers. Applying the experimental value of iT_{11} at $\theta^{\text{LAB}} = 13^0$, which was determined in the previous experiments [22], allows us to obtain the beam polarization P_z. The results obtained for both experimental runs are presented in Table I.

It was checked that in case of applying the full formula describing the $N^\theta_{\text{pol}}(\varphi)$ in the fit procedure, the obtained P_{zz} component was consistent with zero, within the statistical

TABLE I. Values of the vector beam polarization for both experimental runs.

Run number	(P_z, P_{zz})	P_z	ΔP_z^{stat}
1	$(-\frac{2}{3}, 0)$	−0.560	0.018
2	$(-\frac{2}{3}, 0)$	−0.561	0.029

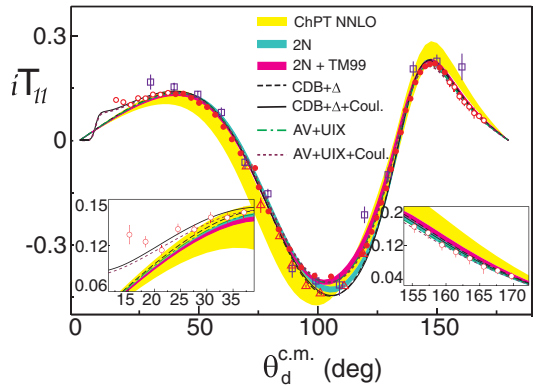

FIG. 1. (Color online) Vector analyzing power iT_{11} for the $d-p$ elastic scattering at 130 MeV: present experiment (red circles), KVI data (full red dots) [22], and earlier data sets: RIKEN data (red triangles) [23] and data from Ref. [24] (violet squares). The investigated areas of the $\theta_d^{\text{c.m.}}$ are enlarged. Theoretical predictions of different approaches are specified by the legend.

error. Next, using the P_z value obtained at one angular point, one can use the above outlined procedure to calculate the elastic scattering analyzing powers iT_{11} at other experimentally covered angles. The obtained results, presented in Fig. 1, form a valuable extension to the data in the area not covered by other experiments.

In the studied region, values of iT_{11} are very small and agree quite well with the theoretical predictions of various approaches. At the very small $\theta_d^{\text{c.m.}}$ angles, one can even deduce the proper trend of Coulomb force corrections to the iT_{11} distribution. In the investigated phase-space region, the data do not reveal any sensitivity to other dynamical effects.

In case of the breakup process, the data were analyzed for a set of geometrical configurations of the two outgoing protons characterized with θ_1, θ_2 between 6° and 12° (with $\Delta\theta = 3°$) and with the relative azimuthal angle φ_{12} from 60° to 180° (with $\Delta\varphi_{12} = 40°$). For each configuration with a given φ_{12}, its "mirror configuration" (i.e., with negative φ_{12}) has been analyzed. In the first step, for each mentioned combinations of angles θ_1, θ_2, and φ_{12} and for polarized and unpolarized states the kinematical spectra E_1 versus E_2 were constructed. Then, the events grouped around the kinematical curve were divided into ΔS bins having widths of 16 MeV and projected on the central kinematics. For a given S bin in the selected configuration, the numbers of the breakup events as a function of the azimuthal angle φ_1 have been determined. The width of φ_1 bin was chosen to be 20°. The obtained numbers of events were normalized to the beam current, corrected for the dead time, and scaled by an adequate trigger downscaling factor.

In the next step, the ratios, similar to the ones introduced in the elastic scattering analysis, were built for each S bin:

$$f^{\xi}(\varphi_1) = \frac{N^{\xi}_{\text{pol}}(\varphi_1) - N^{\xi}_{0}(\varphi_1)}{N^{\xi}_{0}(\varphi_1)}, \tag{4}$$

where (ξ, φ_1) defines a given kinematical point $(\theta_1, \theta_2, \varphi_{12}, S, \varphi_1)$ and $N^{\xi}_{\text{pol}}(\varphi_1)$, $N^{\xi}_{0}(\varphi_1)$ denote the numbers of events for polarized ($P_z = -\frac{2}{3}$, $P_{zz} = 0$) and unpolarized ($P_z = 0$, $P_{zz} = 0$) beam states, respectively.

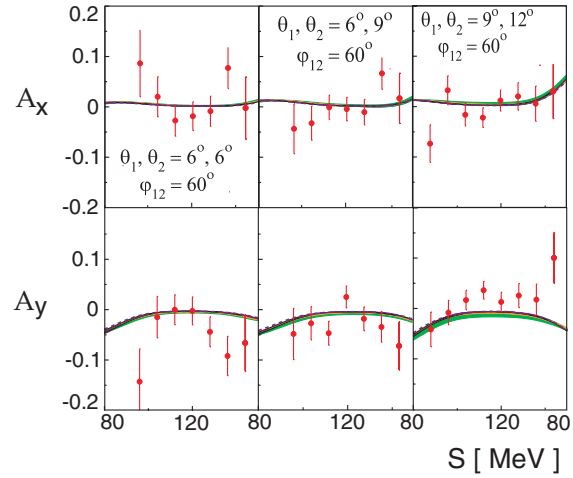

FIG. 2. (Color online) Examples of the $d-p$ breakup vector analyzing powers A_x and A_y for the same relative azimuthal angle $\varphi_{12} = 60°$ and for three different combinations (θ_1, θ_2) of the two coincident protons, specified in the upper panels. Green and orange bands represent calculations based on the chiral theories (at N2LO and N3LO, respectively) and the dashed maroon line shows the calculations based on the realistic AV18 potential combined with the Urbana IX 3NF. The rest of the bands and lines are the same as in the Fig. 1.

The $f^{\xi}(\varphi_1)$ dependency for a pure vector polarized beam state is given by the formula:

$$f^{\xi}(\varphi_1) = \tfrac{3}{2} P_z [A_y(\xi)\cos\varphi_1 - A_x(\xi)\sin\varphi_1]. \tag{5}$$

The values of A_x and A_y can be extracted in a very simple way if one computes combinations of $f^{\xi}(\varphi_1)$ obtained separately for $+\varphi_{12}$ and $-\varphi_{12}$ (taking advantage of the parity restrictions):

$$f^{\xi}(\varphi_1, +\varphi_{12}) - f^{\xi}(\varphi_1, -\varphi_{12}) = -3P_z A_x(\xi)\sin\varphi_1, \tag{6}$$

$$f^{\xi}(\varphi_1, +\varphi_{12}) + f^{\xi}(\varphi_1, -\varphi_{12}) = 3P_z A_y(\xi)\cos\varphi_1. \tag{7}$$

Using the beam polarization P_z obtained from the elastic scattering analysis, the breakup vector analyzing powers were evaluated from linear fits of the above combinations of f^{ξ} as functions of the sine or cosine of the first proton azimuthal angle φ_1, respectively. A_x and A_y have been evaluated for 48 kinematical configurations, resulting in about 300 data points. Examples of the A_x and A_y distributions in the function of S obtained for three configurations are presented in Fig. 2. The obtained vector analyzing power data were compared to the state-of-the-art theoretical calculations.

In order to quantitatively inspect the description of the whole data set provided by various models, the values of χ^2 per degree of freedom (d.o.f.) have been calculated for A_x and A_y for each type of the theoretical prediction. In case of the theoretical results presented in the figures as bands, the χ^2 values were calculated with respect to the center of the band. For A_x all values of χ^2/d.o.f. agree with each other and are around 0.6. For A_y, the obtained values of χ^2/d.o.f are higher, around 1.8, independent of the considered theoretical prediction. This fact indicates that the calculational approaches in this case are less successful in describing the data.

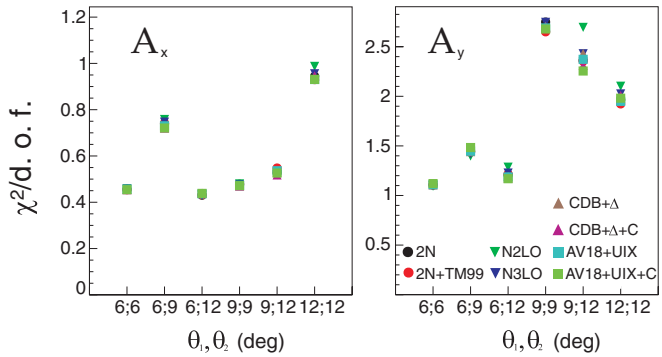

FIG. 3. (Color online) Quality of description of the vector analyzing power data with various predictions (defined in the legend), expressed as χ^2/d.o.f. dependence on combination of the proton emission polar angles.

The analysis was also performed with respect to kinematical variables: The energy of the relative motion of the two protons E_{12}, relative azimuthal angle φ_{12} of the breakup protons, and pair of the polar angles of the two protons θ_1, θ_2 (see Fig. 3). The obtained results for both observables are distributed rather randomly with respect to the χ^2/d.o.f. values for each of the kinematical variable, and no significant difference between the theoretical predictions is observed. One can conclude that the results are quite consistent with one another, considering various theoretical calculations for both of the observables.

The obtained values of the A_x and A_y analyzing powers are very small, and they do not reveal any interesting effect connected with the 3N dynamics. In general, the data confirm all the theoretical models, though they can be described by the calculations limited to the pairwise NN interaction only.

This work was partially supplemented by the Polish 2008–2010 science funds as Research Project No. N N202 174635 and by the Polish 2009–2011 science funds as Research Project No. N N202 034836.

[1] S. A. Coon and H. K. Han, Few-Body Syst. **30**, 131 (2001).
[2] B. S. Pudliner *et al.*, Phys. Rev. C **56**, 1720 (1997).
[3] A. Deltuva, R. Machleidt, and P. U. Sauer, Phys. Rev. C **68**, 024005 (2003).
[4] E. Epelbaum *et al.*, Phys. Rev. C **66**, 064001 (2002).
[5] A. Deltuva, A. C. Fonseca, and P. U. Sauer, Phys. Rev. C **71**, 054005 (2005).
[6] A. Deltuva, A. C. Fonseca, and P. U. Sauer, Phys. Rev. C **73**, 057001 (2006).
[7] A. Deltuva, Phys. Rev. C **80**, 064002 (2009).
[8] H. Witala, W. Glockle, D. Huber, J. Golak, and H. Kamada, Phys. Rev. Lett. **81**, 1183 (1998).
[9] S. Nemoto, K. Chmielewski, S. Oryu, and P. U. Sauer, Phys. Rev. C **58**, 2599 (1998).
[10] H. Sakai *et al.*, Phys. Rev. Lett. **84**, 5288 (2000).
[11] K. Ermisch *et al.*, Phys. Rev. Lett. **86**, 5862 (2001).
[12] K. Hatanaka *et al.*, Phys. Rev. C **66**, 044002 (2002).
[13] R. V. Cadman *et al.*, Phys. Rev. Lett. **86**, 967 (2001).
[14] K. Ermisch *et al.*, Phys. Rev. C **71**, 064004 (2005).
[15] P. Mermod *et al.*, Phys. Lett. B **597**, 243 (2004).
[16] K. Sekiguchi *et al.*, Phys. Rev. C **65**, 034003 (2002).
[17] K. Sekiguchi *et al.*, Phys. Rev. C **70**, 014001 (2004).
[18] St. Kistryn *et al.*, Phys. Rev. C **68**, 054004 (2003).
[19] St. Kistryn *et al.*, Phys. Rev. C **72**, 044006 (2005).
[20] E. Stephan *et al.*, Phys. Rev. C **82**, 014003 (2010).
[21] M. Betigeri *et al.*, Nucl. Instrum. Methods Phys. Res., Sect. A **421**, 447 (1999).
[22] E. Stephan *et al.*, Phys. Rev. C **76**, 057001 (2007).
[23] H. Mardanpour *et al.*, Eur. Phys. J. **31**, 383 (2007).
[24] H. Witała *et al.*, Few-Body Syst. **15**, 67 (1993).